On the underpotential-overpotential transition in the deposition of bismuth on a smooth polycrystalline platinum electrode

Antanas Steponavičius, Laima Gudavičiūtė, Violeta Karpavičienė and Vidmantas Kapočius

Institute of Chemistry, A. Goštauto 9, LT-2600 Vilnius, Lithuania

The deposition of bismuth onto a smooth polycrystalline Pt electrode from acidic perchlorate solutions was investigated over a wide range of potentials, covering both underpotential and overpotential regions, by means of linear sweep voltammetry (LSV), cyclic voltammetry (CV) and potential step techniques. The bismuth adsorption isotherm onto platinum was evaluated. On the basis of potentiostatic current transients, it was shown that the early stages of deposition of Bi on Pt quite well fit the progressive mechanism of 3D nucleation and growth under diffusion control. Some nucleation parameters were evaluated, depending on the experimental conditions.

Key words: bismuth, platinum elctrode, underpotential deposition, overpotential deposition, initial stages, perchlorate solution

INTRODUCTION

The properties and state of electrode/solution interface exert a profound influence on the rate of nucleation and growth of a new phase (see, *e. g.*, [1] and the references cited therein). Thus, the study of initial stages of electrocrystallization of metals (M) on different substrates (S) are of significant theoretical importance for the elucidation of the kinetics and mechanism of M electrodeposition.

The overall technological evolution is strongly associated with the development of new materials and with the extension of their practical implementation. Considerable promises seem to be associated with bismuth. In recent years, the progress in its use for various theoretical and practical purposes has been rather rapid. In particular, Bi in a submonolayer range on various S is widely used for electrocatalysis of numerous redox reactions (see, *e. g.*, review works [2–6]).

Bi thin films offer for exploring not only the intricate transport properties of semimetals, but for technological applications in wide-range field and current sensors, owing to Bi unusual electronic properties.

The underpotential deposition (UPD) of Bi onto various S is well documented in a number of papers [7–22], whereas to our knowledge, there is no investigation of the early stages of Bi electrodeposition.

The present paper deals with the underpotential-overpotential transition phenomena on deposition of Bi onto a smooth polycrystalline Pt electrode from acidic solution in order to characterize the nucleation and growth mechanism in the overpotential range.

EXPERIMENTAL

0.01–0.9 mM Bi^{3+} solution in 0.5 M H_2SO_4 (measurements in the UPD zone) and 0.05 or 0.1 M Bi^{3+} solutions in $HClO_4$ (measurements in the OPD zone) were used in our experiments. Bi^{3+} exhibits a tendency toward hydrolysis, but in strongly acidified solutions the Bi^{3+} ion was shown not to hydrolyze [23].

The working solution (WS) for the measurements in the UPD zone was prepared as described elsewhere [22]. The WS for the measurements in the OPD zone was prepared by dissolution of $Bi(ClO_4)_3$ in $HClO_4$ (both reagents of the highest purity). Prior to each experiment the WSs were deaerated with Ar for 1 h.

All experiments were performed at 20 ± 0.1 °C in a JASE-2 three-electrode thermostated electrochemical cell (made in Belarus). The working electrode (WE) was a vertical disc made from a mat polycrystalline Pt foil (99.99% purity) and sealed into a soft glass tube. The geometric area of the WE was 1 cm^2. The real electrode surface area was determined from the hydrogen adsorption voltammetric profile recorded at 50 mV s^{-1} in 0.5 M H_2SO_4 solution, taking the theoretical hydrogen adsorption charge of

210 μC cm^{-2} as noted in [24, 25]. The roughness factor (*f*) was found to be equal to 2.8 ± 0.1 (measurements in the UPD range) or 2.0 ± 0.1 (CV and *E* steps in the OPD zone). Separate experiments were also carried out using a bulk Bi electrode, 1 cm^2 in area. The counter electrode was a Pt sheet of *ca*. 6 cm^2 in area. The reference electrode was an Ag/AgCl/KCl(sat.) electrode. All potentials (*E*) in the text are referred to the SHE scale. Unless otherwise noted, all currents (*i*) and charges (*Q*) are reported with respect to the geometric area of the WE.

The pretreatment of the Pt WE and the checking of the quality of this pretreatment were carried out as described in [22]. Between the runs the cell and accessory components were cleaned with warm concentrated H_2SO_4, rinsed repetitively with doubly distilled water and left in it overnight.

A linear sweep voltammetry (LSV) and cyclic voltammetry (CV) were performed using a PI 50-1 potentiostat, a PR-8 programmer and an LKD-003 X-Y recorder (all made in Belorus). The CV curves (CVs) were recorded after a steady-state *i*/*E* profile was obtained in the quiescent WS. In separate experiments, the effect of a repetitive cycling was also monitored. Unless otherwise stated, the WE was allowed to stand at the open-circuit potential (OCP ≈ 0.80 ± 0.02 V) for 3 min, and afterwards the *E* cycling started from OCP in the negative direction. In the present work, the equilibrium potential (E_{eq}) for the Bi/Bi^{3+} couple was not calculated. The experimental value E_{eq} was evaluated by experiments using the Bi WE.

The chronoamperometric measurements were carried out using a PI 50-1 potentiostat, interfaced through a home-made analogue to a digital converter with a PC (Siemens) and a PR-8 programmer. The potentiostatic *i*/*t* traces were recorded starting with a potential (E_{start}) in the UPD zone. First the Pt WE was kept at the selected E_{start} for 5 min, and then *E* was stepped to the OPD zone to obtain a chosen overpotential (η_c) with respect to the E_{eq}. The experimental data acquisition was in a numerical form with time resolution of 4 or 50 ms per point. After disconnecting the electronic circuit of the potentiostat, the Bi-covered Pt WE was left in the WS until its *E* approached spontaneously the value of ≈ +0.8 V. Then the remaining amount of Bi deposit was desorbed oxidatively by polarization at +1.30 V for 1 min and by immersion into HNO_3 (1:1) solution for 5 min. Thereafter, the WE was rinsed with doubly distilled water and finally transferred into another cell with 0.5 M H_2SO_4 solution to be subjected to a repetitive cycling at 50 mV s^{-1} between +1.30 and +0.05 V, until the *i*/*E* profile characteristic of a clean Pt electrode was recorded. Each experiment with the *E* step was preceded by this pretreatment of the Pt WE.

RESULTS AND DISCUSSION

1. Underpotential deposition of Bi onto Pt from sulphate solution. The UPD processes involve three different kinds of interaction emerging between respective elements taking place in these processes. The first interaction emerges between the surface of S and an atom deposited underpotentially, the second one between the UPD atom and an anion in the supporting electrolyte, and the third one between the surface of S and the anion. Therefore, it seems reasonable to make some comments on both the electrochemical behaviour of Pt in acidified sulphate solutions and the inferred effect of specific adsorption of anion on the Bi adlayer formation.

The adsorption of sulphate (in a general sense, SO_4^{2-} and HSO_4^- species) onto Pt in metal ion-free solution has been investigated intensively in the recent years. Some comments on this matter have been briefly presented in [22]. HSO_4^- and SO_4^{2-} were shown to be specifically adsorbed onto Pt surface. This adsorption is strongly governed by both the *E* window and structural characteristics of the S surface. As far as we know, rather little attention, however, has been paid to the formation of Bi and (bi)sulphate coadsorbate structures onto Pt surface. Particularly, it was found that the presence of Bi adatoms in advance adsorbed irreversibly onto Pt(111) electrode (this adsorption occurs due to immersion of Pt in Bi(III) solution in the absence of external voltage) led, at *E* scan, to a diminution of the total *Q* involved in the adsorption/desorption of hydrogen and sulphate species [15, 18, 20]. To our knowledge, no similar investigation, however, was undertaken for a polycrystalline Pt electrode. In addition, it should be mentioned that no specific adsorption of SO_4^{2-} anion was established on a bulk Bi electrode [26]. So, in the light of these considerations, one might reasonably assume that, under conditions of our experiment, any complications expected due to the coadsorption of Bi and (bi)sulphate species onto a polycrystalline Pt should be rather insignificant, especially at higher coverages by Bi (θ_{Bi}).

The UPD of Bi on the polycrystalline Pt WE is shown in Fig. 1, where the potential sweep curves are given for Pt in the absence and in the presence of Bi^{3+} for two sweep rates (*v*) for comparison. A profound difference between the curves recorded in the absence and in the presence of Bi^{3+} is observed. In each case, the reduction of surface platinum oxide, peak c3, is followed by the Bi UPD. Namely, an increase in the current at *E* in the region of this peak gives an additional charge density flow which amounts to *ca*. 70% of the total charge density flow over the whole *E* region under study, as shown in

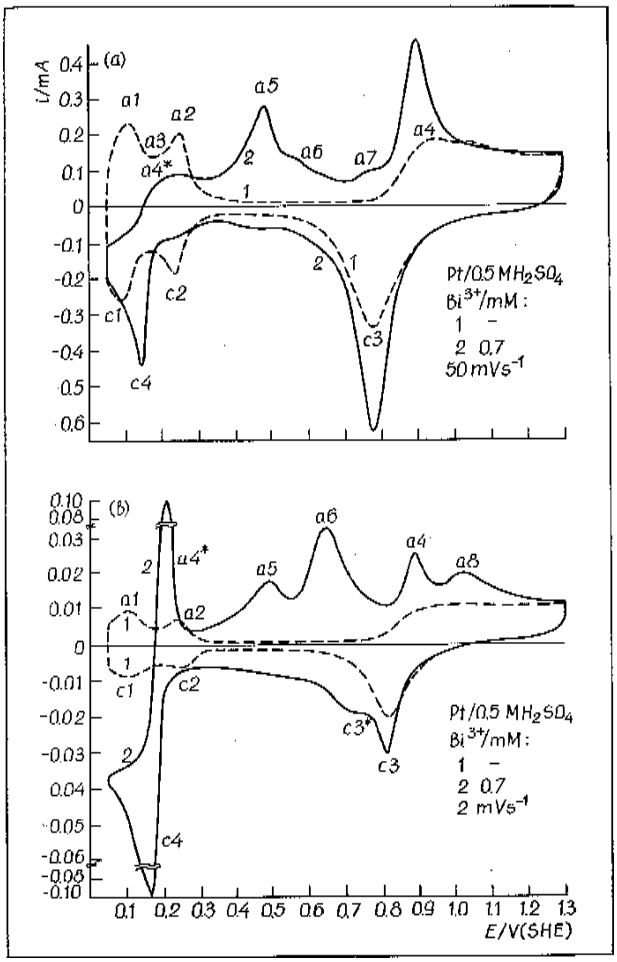

Fig. 1. Stabilized cyclic voltammograms for a polycrystalline Pt electrode in 0,5 M H_2SO_4 solutions without (1) or with Bi^{3+} (2) at 50 (*a*) or 2 (*b*) mV s^{-1}

[22]. The current peaks c1 and c2 corresponding to the hydrogen adsorption become suppressed. Bi shows a sharp oxidation peak a4 at the onset of oxide formation on Pt. A more detailed analysis of the features associated with the Bi UPD/oxidation is given in [22].

Although the *i*/*E* profiles recorded for the Pt electrode in acidic Bi^{3+} sulphate (Fig. 1) and perchlorate [8, 9, 15, 18, 21] solutions (these kinds of solutions were mainly used to investigate the Bi UPD onto Pt) were principally similar, some differences in the voltammetry of the Bi UPD could also be marked out [22]. It was shown, for example, that more pronounced differences were associated with the cathodic current peak c3 which appeared due to reduction of surface platinum oxide (Fig. 1). In particular, while an increase in i_{pc3} alone and the negative shift of its potential in the presence of Bi^{3+} were established in perchlorate solutions [9, 10], a non-linearity of the relationship of i_{pc3} with the bulk concentration of Bi^{3+} and an invariance of the position of E_{pc3} with increasing *c* were revealed for sulphate solutions [22]. In addition, resolution of an additional shoulder c3* on the *i*/*E* curve recorded at a low sweep rate (*e. g.*, at 2 mV s^{-1}, as shown in Fig. 2*b*, curve 2) became possible for sulphate solution.

Continuing to investigate the formation of the Bi adlayer onto Pt in acidic Bi^{3+} sulphate solution, the *E* step technique was also used here. The typical potentiostatic current transients are shown in Fig. 2. To obtain the values of Q_c which might be considered as those involved in the Bi UPD, a set of such current transients was analyzed with respect to the bulk *c* of Bi^{3+} and E_{start}. The Q_c from different *E* steps are presented in Fig. 3*a*, depending on the bulk *c* of Bi^{3+} and E_{start}. The Q_c obtained here are, in principle, rather close to the accumulated Q_c calculated earlier on the basis of CVs [22].

Then, the charge, which can be related to the Bi UPD only, is formally taken as the difference $(Q_c^{Bi}–Q_c^{0})$, where Q_c^{0} and Q_c^{Bi} are the charges calculated from the current transients in the absence and in the presence of Bi^{3+} in 0.5 M H_2SO_4 solution, respectively. The $(Q_c^{Bi}–Q_c^{0})$ *vs*. *E* plots are shown in Fig. 3*b*. As is seen, the charge *vs*. *E* curves differs in shape depending on the value of E_{start}. The experimental magnitude of charge which is assumed here to be associated with the Bi UPD is markedly higher when E_{start}. = +1.20 V; *e. g.*, at *E* = +0.50 V this quantity is about 5 times higher than at E_{start}.= +0.80 V. This fact rather well correlates with the CV measurements by Cadle and Bruckenstein who showed that the Bi UPD could be associated with the simultaneous occurrence of two reduction processes, *viz*., the reduction of Bi(III) species irreversibly adsorbed in the range of the more positive *E* and the reduction of sur-

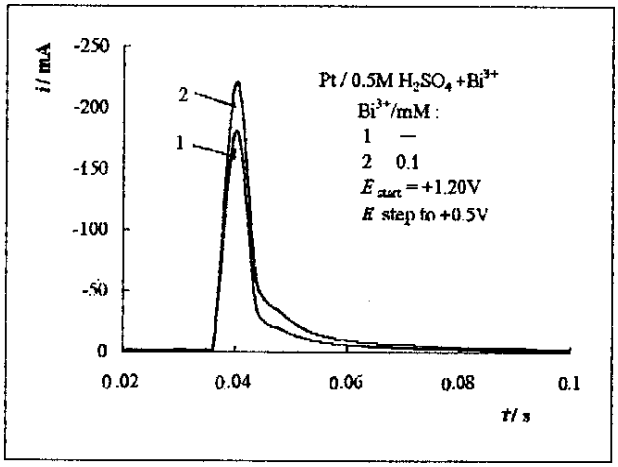

Fig. 2. Potentiostatic current transients recorded for a smooth polycrystalline Pt electrode in acidic Bi^{3+} sulphate solution

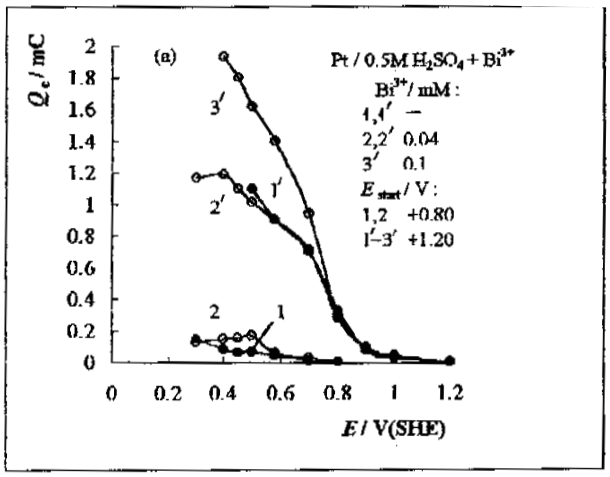

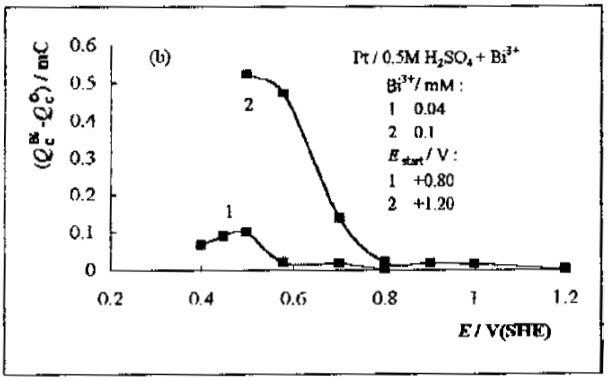

Fig. 3. Potential-dependences of cathodic charges Q_c derived from the current transients depending on the starting potential and bulk concentration of Bi^{3+} (*a*) and of difference ($Q_c^{Bi} - Q_c^{o}$), where Q_c^{o} and Q_c^{Bi} are the charges in the absence and in the presence of Bi^{3+} (*b*) in acidic sulphate solution

face platinum oxide [9], and with the observation that the main part of charge consumed for the Bi(III) reduction to Bi(0) over the whole range of underpotentials belongs to the region of peak c3, as shown in [22]. At the same time, it should be noted that, in the present study, the charge *vs*. *E* curve (Fig. 3*b*, curve *2*) is shifted toward the more negative *E* by ca. 100 mV and therefore somewhat correlates with the appearance of a shoulder observed on the CV under the quasi-steady conditions of electrolysis of Bi^{3+} sulphate solution in the region of peak c3 (Fig. 1*b*, curve *2*). It should be also emphasized that taking into account the roughness factor of the Pt WE and also the calculated number of platinum surface sites occupied by one Bi adatom (S = 3, as shown in [12]), the results represented by curve 2 in Fig. 3*b* at E = +0.50 V are quite close to the expected values for the three-electron process.

2. Voltammetry of Pt and Bi-covered Pt electrodes in acidic Bi^{3+} perchlorate solutions. As far as we know, there is almost no experimental material on the voltammetry in a system when Pt electrode becomes covered with Bi from a strongly acidic Bi^{3+} solution. The typical *i*/*E* curves recorded by a single triangular *E* sweep for the Pt WE are shown in Fig. 4. They have a rather sharp peak of bulk Bi electrodeposition in the cathodic half-cycle from the acidic perhlorate solutions which will be used to study the early stages of the electrocrystallization of Bi. The steepness of the rising portion of *i*/*E* curves suggests the reversibility of the electrode reaction occurring at *E* in the OPD zone. As can be seen, some features of the potentiodynamic *i*/*E* profiles in the cathodic half-cycle, in particular, the *v*-depen-

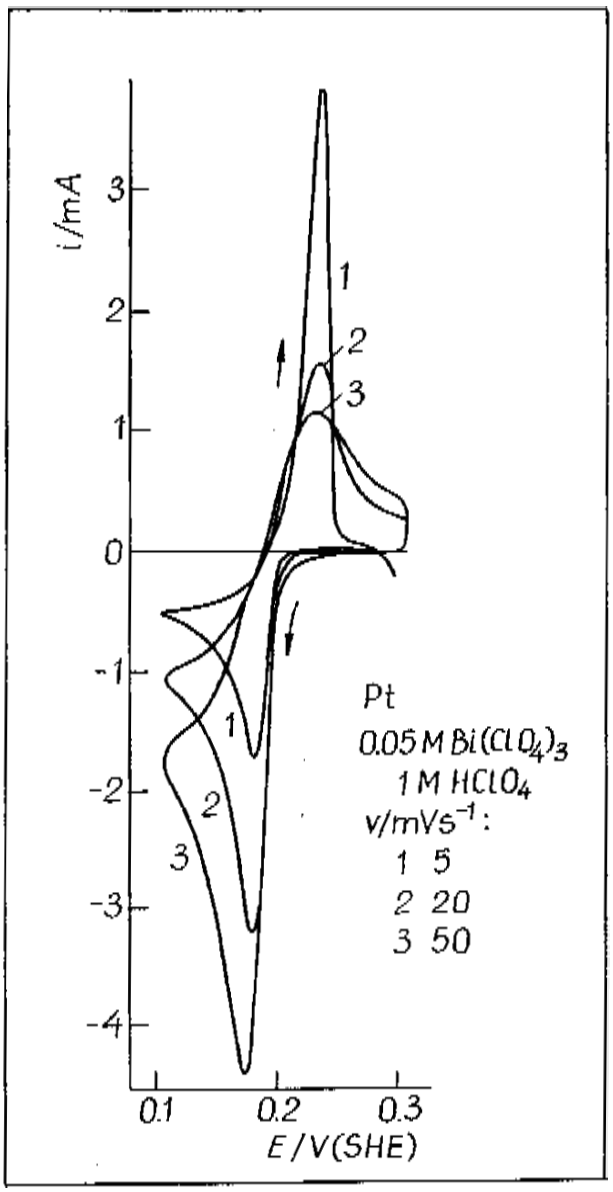

Fig. 4. Single sweep curve for a smooth polycrystalline Pt electrode in 1 M $HClO_4$ + 0.05 M $Bi(ClO_4)_3$ solution at potential sweep rate *v*: *1* – 5, *2* – 20 and *3* – 50 mV s^{-1}. Potential sweep started from E_{start} = +0.30 V

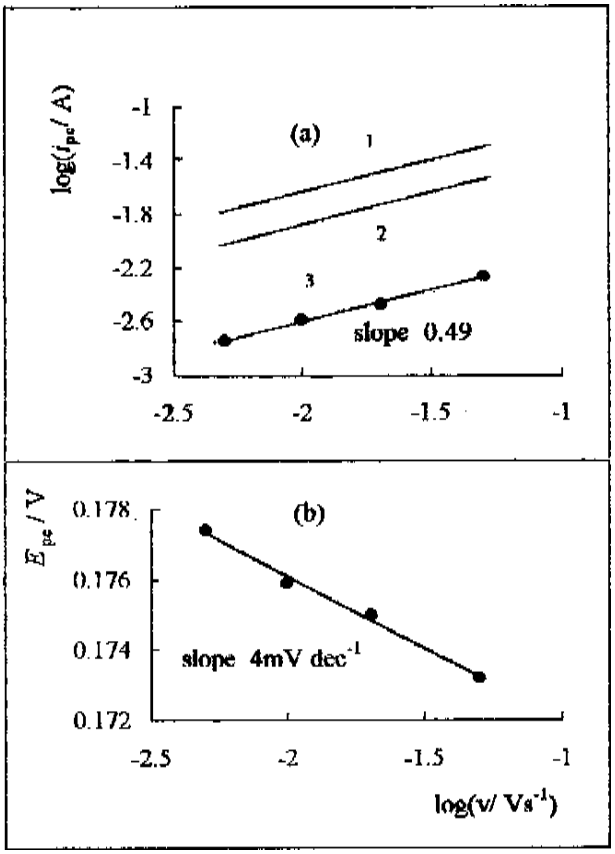

Fig. 5. Dependences of cathodic current peak height (*a*) and peak potential (*b*) on the potential sweep rate in 1 M $HClO_4$ + 0.05 M $Bi(ClO_4)_3$ solution. In part (*a*): *1* – calculated line for a reversible process, *2* – the same for an irreversible process, *3* – experimental data (from. Fig. 4)

dences of both current peak height i_{pc} and peak potential E_{pc} (Fig. 5), the passage of the i_{pc} *vs.* $v^{0.5}$ plot through the origin and also the E_{pc} and the half-peak potential separation $|E_{pc/2}–E_{pc}|$ being equal to 0.0175 V for curve 3 (Fig. 4), formally fit the quantities expected for the reversible electrode reaction [27]. However, at first sight, the difference in i_{pc} observed experimentally here and calculated for the case of either reversible or irreversible charge transfer (*cf.* curves *1* and *3* in Fig. 5) seems to be rather obscure.

After reversing the potential sweep, the development of anodic current peak is observed (Fig. 4). It is interesting to note that although the anodic peak potential E_{pa} does not depend on v (Fig. 4), the height of the anodic current peak i_{pa} decreases with v. With regard to the complex nature of anodic dissolution of bulk Bi in acidic media [7–9, 22], such a feature of potentiodynamic *i*/*E* curves can be quite explainable.

To conclude, the non-stationary and quasi-steady voltammetric *i*/*E* profiles in the Bi^{3+}-containing acidic system illustrate some features which are still unclear, on the one hand, and also signify roughly the *E* zone for the further investigation of the early stages of Bi electrodeposition onto the polycrystalline Pt electrode.

3. Investigation of the early stages of Bi electrodeposition on a smooth polycrystalline Pt electrode in acidic perchlorate solution. The potentiostatic current transients for the bulk Bi deposition, obtained by the *E* steps from various E_{start}, all being in the UPD zone (*cf.* Fig. 1), to various η_c (cf. Fig. 4) are shown in Figs. 6–8. Most of these transients have a shape expected for 3D deposition process with diffusion control [28]. In particular, at a very short time (t < 0.1 s) a sharp peak is observed due to both a double layer charging and probably to an as yet unknown additional process (*e. g.*, formation of Bi adlayer or Bi reduction intermediates) (Fig. 7). As an illustration, this charge was calculated to be equal to *ca*. 1.61 mC or, taking into account $f \approx 2.0$, to *ca*. 0.80 mC cm^{-2} when the *E* was stepped from

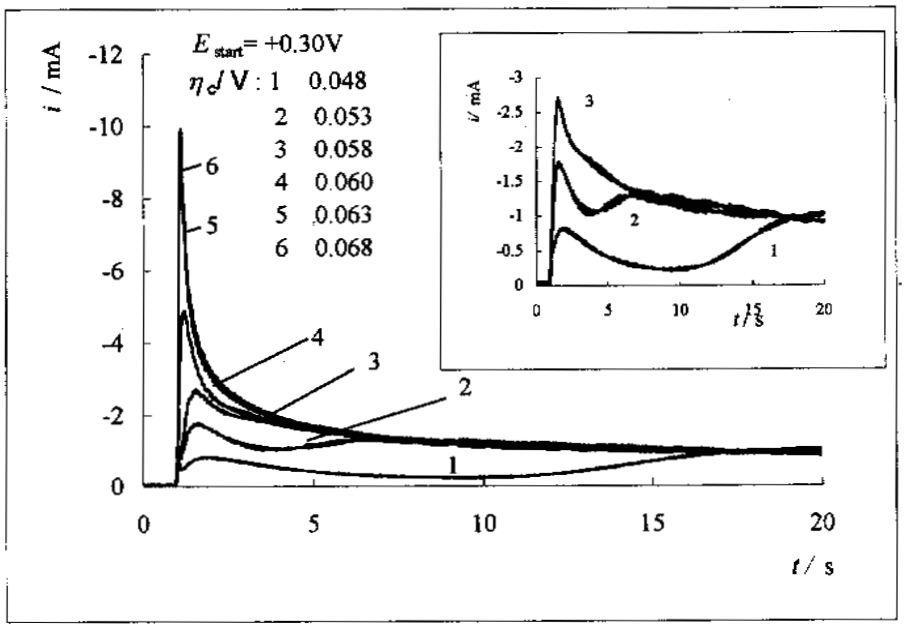

Fig. 6. Potentiostatic current–time transients depending on the stepped value of potential for Pt electrode in 1.0 M $HClO_4$ + 0.1 M $Bi(ClO_4)_3$ solution. E_{start} = +0.30 V, E_{eq} for the Bi/Bi^{3+} couple is equal to +0.238 V. Inset illustrates the shape of current–time transients in an enlarged scale

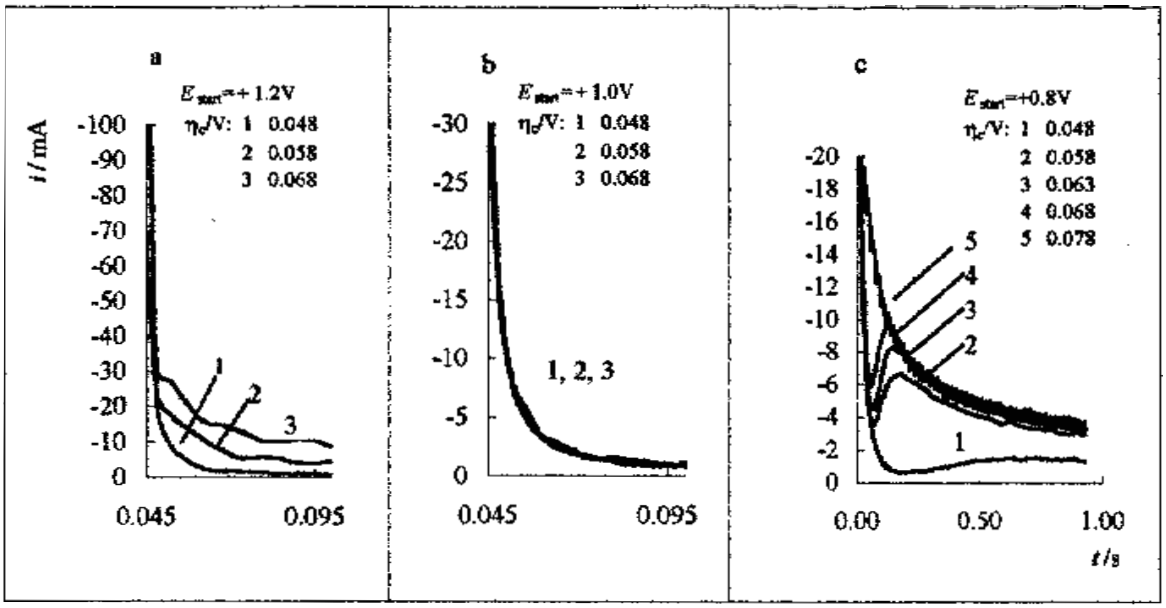

Fig. 7. Potentiostatic smoothened current–time transients depending on the overpotential for Pt electrode in 1.0 M $HClO_4$ + 0.1 M $Bi(ClO_4)_3$ solution. E_{start}: +1.20 (*a*), 1.0 (*b*) and +0.80 V (*c*), E_{eq} = +0.238 V

+0.80 V to η_c = 0.048 V. Such a value of charge density is more than trebly as large as that required for the complete coverage by Bi adlayer of the polycrystalline Pt electrode at θ_{Bi} = 0.33 [12, 22], but it seems to formally approach that consumed in the case of the so-called compressed Bi overlayers [18]. This does not necessarily mean that one monolayer of Bi is actually formed. This charge is, however, far in excess of that required to recharge the double layer. In the succeeding part of *i*/*t* transients, *i* rises to a maximum with *t*, and then the curves tend to merge into one, reflecting the diffusion limitations described by Cottrell's equation. For such a

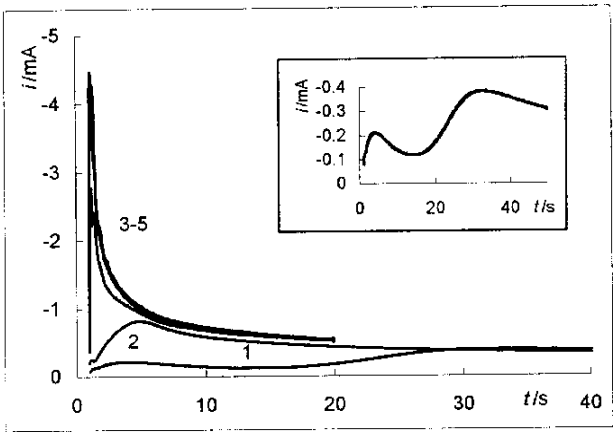

Fig. 8. Potentiostatic current–time transients depending on the overpotential for Pt electrode in 1.0 M $HClO_4$ + 0.05 M $Bi(ClO_4)_3$ solution. E_{start} = +0.30 V, E_{eq} = +0.234 V. Overpotential: *1* – 0.044, *2* – 0.049, *3* – 0.054, *4* – 0.058 and *5* – 0.064 V. Inset shows the *i*/*t* profile at overpotential of 0.044 V in an enlarged scale to depict two waves

3D nucleation with diffusion control, the theory of Scharifker and Hills [28] provides two limiting cases, depending on the nucleation rate.

In the first case, at high nucleation rates, all nuclei are formed immediately after the *E* step and their number remains constant during the growth process. This case is considered as instantaneous nucleation and is described by [28]:

$$i(t) = [zFD^{0.5}\ c/(\pi t)^{0.5}]\cdot\ [1–\exp(–N\pi kDt)], \qquad (1)$$

where $i(t)$ is the current normalized by the geometric area of the electrode surface, *N* is the total number of the formed nuclei (in cm^{-2}), *k* is the numerical constant determined by the conditions of the experiment:

$$k = (8\pi cM/\rho)^{0.5}, \qquad (2)$$

M and ρ are the molecular weight and the density of the deposited M, respectively, *zF* is the value on the molar charge of the electrodepositing species, *D* is the diffusion coefficient, *c* is the bulk concentration (in mol cm^{-3}).

The second case, at small nucleation rates, when the nuclei are continuously formed during the whole process, is called progressive nucleation [28]. In this case, the M clusters of different sizes can be formed, especially at the very initial *t*. The current transient for progressive 3D nucleation-growth mechanism is given by [28]:

$$i(t) = [zFD^{0.5}c/(\pi t)^{0.5}]\cdot[1–\exp(–aN_0\pi k'Dt^2/2)], \qquad (3)$$

where N_0 is the number density of S active sites (in cm^{-2}), a is the steady state nucleation rate constant per site, k' is again a numerical constant given by

$$k' = (4/3)(8\pi cM/\rho)^{0.5}. \quad (4)$$

The very initial stages in the M deposition process on foreign S are usually examined beginning with an analysis of the i/t transients, including the rising part of these curves [28–32]. In the present work, however, this kind of analysis is somewhat complicated, because the process to be studied is likely accompanied by other process which might have a certain contribution in i at $t < t_{max}$. Therefore, to distinguish between the two mechanisms mentioned above, along with the widely used analysis of the i/t curve, the transient plotted in reduced variables $(i/i_{max})^2$ *vs.* (t/t_{max}) can be also applicable [28]. In that event, quite a strict test for fitting the experimental data with the models of instantaneous or progressive nucleation-growth should be made by comparing the recorded transients transformed into reduced variables with those calculated according to theoretical equations [28] – for instantaneous nucleation:

$$(i/i_{max})^2 = 1.9542(t/t_{max})^{-1}\cdot\{1-\exp[-1.2564(t/t_{max})]\}^2 \quad (5)$$

and for progressive nucleation:

$$(i/i_{max})^2 = 1.2254(t/t_{max})^{-1}\cdot\{1-\exp[-2.3367(t/t_{max})^2]\}^2. \quad (6)$$

Figure 9 shows such a presentation of the $(i/i_{max})^2$ *vs.* (t/t_{max}) plots for different E_{start} and η_c. As can be seen, the experimental data rather well fit those for the progressive mechanism calculated according to Eq. (6). Although there is a certain scattering of the experimental points in the rising part of the curves (Fig. 9), which is known [28] to be crucial for the calculation of the nucleation rate, it seems that this portion of the experimental data is also suitable for the further considerations.

As can be seen from Eq. (3), the i/t response is determined both by such parameters of depositing species as its c and diffusion coefficient D, on the one hand, and by the parameter of deposition process as such, namely, the nucleation rate aN_0, on the other hand. At the same time, the product $i^2_{max}\cdot t_{max}$ is independent of the quantity aN_0. So, this product can be used to evaluate the D, if the bulk c of M ion is given. Then, according to the equation [28]:

$$i^2_{max}\cdot t_{max} = 0.2598(zFc)^2D, \quad (7)$$

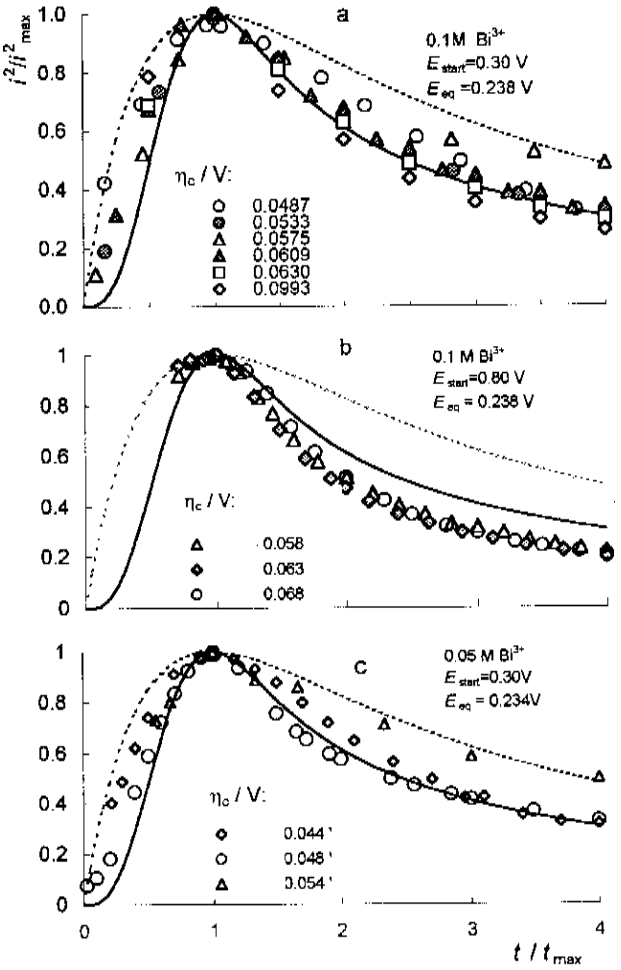

Fig. 9. Reduced-variable i^2/i^2_{max} *vs.* t/t_{max} plots of the transients: *a* – from Fig. 6, *b* – from Fig. 7*b* and *c* – from Fig. 8. Calculated curves for instantaneous (dotted line) and progressive (full line) nucleation are also shown. In part (*c*) the second current wave was used

D for Bi^{3+} was obtained to be by about two orders of magnitude less than the value characteristic of the diffusion of ions in aqueous solutions. Such a phenomenon is not yet fully understood. However, in our opinion, among the possible reasons for this finding, the complication of the Bi nuclei growth process due to a slow surface diffusion of Bi adatoms seems to be rather plausible. For example, the surface diffusion coefficients (D_{surf}) of such an order are considered in a comparative study of the early stages of electrodeposition of various M on columnar and smooth Pt electrodes [33]. Following the cited work, an evaluation of the D_{surf} from the ratio of M melting temperature to ambient temperature will result in D_{surf} of $3.8\cdot10^{-7}$ cm^2 s^{-1} for Bi adatom. In the present study, the experimental value of $D = 8\cdot10^{-8}$ cm^2 s^{-1} was further used for the calculation of the Bi deposition parameters (this value was obtained from Eq. (7); a rather close value was also obtained from the Cottrellian region of transients).

An important parameter in the kinetics of nucleation processes is the critical number of atoms in the stable nuclei (N_{crit}) [1, 34, 35]. As is customary [1, 34, 35], N_{crit} can be evaluated in several ways, for example: (*i*) from the critical free energy, when all kinds of the interactions between the respective components involved in the process are taken into account; (*ii*) according to the so-called atomistic "small cluster model", from the η_c-dependence of the nucleation rate aN_0, when nucleation is considered as a sequence of bimolecular reactions in which every cluster transforms into the next one by attachment or detachment of one atom. In the latter case, N_{crit} is calculated from the $\ln(aN_0)$ *vs.* η_c plot [1]:

$$N_{crit} = (RT/zF)\cdot[\mathrm{d}\ \ln(aN_0)/\mathrm{d}(\eta_c)]. \qquad (8)$$

Such experimental plots are presented in Fig. 10. From the respective slopes it follows that N_{crit} here depends on both the bulk c of Bi^{3+} and E_{start}, *viz.* at

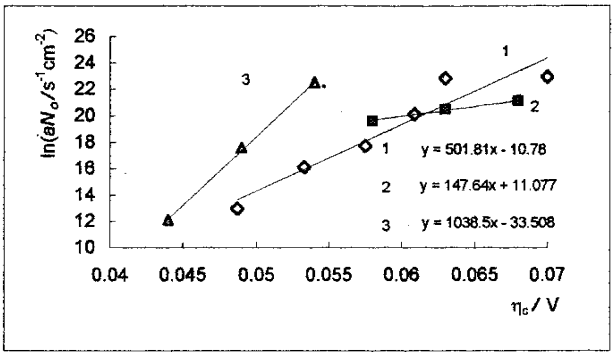

Fig. 10. Variation of the nucleation rate on the overpotential for the pc Pt electrode in 1.0 M $HClO_4$ + 0.1 M $Bi(ClO_4)_3$ solution (*1, 2*) at E_{start} = +0.30 V (*1*) or +0.80 V (*2*), and in 1.0 M $HClO_4$ + 0.05 M $Bi(ClO_4)_3$ solution at E_{start} = +0.30 V (*3*)

c = 0.1 M Bi^{3+} N_{crit} is equal to 4–5 or *ca.* 1, when E step started from +0.30 or +0.80 V respectively, and at c = 0.05 M Bi^{3+} this quantity is equal to 8–9, when E_{start} = +0.30 V. So, as can be seen, in the η_c range studied the N_{crit} value was found to be significantly smaller in the case of E_{start} = +0.80 V than at E_{start} = +0.30 V. This may not be too surprising in view of the observations ([22] and Fig 3*b*) that the former E_{start} value lies outside the E range where the formation of Bi adlayer onto Pt electrode can be expected, *i.e.* it is thought that starting from +0.80 V the surface of the Pt WE is actually bare. On the other hand, in the case of E_{start} = +0.30 V, a different picture emerges – the formation of the Bi submonolayer becomes possible ([22] and Fig. 3*b*). Then, taking into account the known difference in the interactions between the Pt–Bi_{ad} at underpotentials and Bi_{ad}–Bi at overpotentials, where Bi represents the Bi atom during the first stages of electrocrystallization, it is conceivable that even a single Bi adatom deposited onto a relatively bare Pt electrode becomes sufficiently stable to be considered as a nucleus of critical size.

Considering the influence of the bulk c of Bi^{3+} on the parameter aN_0 at the same E_{start}, it seems that the increase in the slope of the $\ln(aN_0)$ *vs.* η_c plot with the dilution of solution (Fig. 10) should be noted, firstly, as a phenomenon. At the same time this finding is suggested to be associated with a relationship between $\ln(aN_0)$ and an initial underpotential (ΔE_i) as shown in [1, 35]. In particular, it has been shown that the parameter $\ln(aN_0)$ tends to rise with the positive shift of E_{start}. In our case, such a change in E_{start} seems to be possibly related with the difference of $|E_{start} - E_{eq}|$. Then, from the strong Bi–Pt interaction and a significant positive Bi–Pt lattice misfit ($d_{0,Bi} > d_{0,Pt}$), and according to the con-

Table. **The nucleation rate (aN_o) and maximum possible surface saturation with nuclei Bi (N_{sat}) in Bi^{3+} perchlorate solutions onto the smooth polycrystalline Pt electrode. t^0 = 20 °C**

Solution	E_{start} / V	Overpotential / V	aN_o / $s^{-1}cm^{-2}$	N_{sat} / cm^{-2}
0.1 M $Bi(ClO_4)_3$ + 1 M $HClO_4$	0.3	0.049	$4.26\cdot10^5$	$3.8\cdot10^6$
		0.053	$9.83\cdot10^6$	$1.8\cdot10^7$
		0.057	$4.97\cdot10^7$	$4.1\cdot10^7$
		0.061	$5.40\cdot10^8$	$1.4\cdot10^8$
		0.063	$8.29\cdot10^9$	$5.3\cdot10^8$
		0.070	$9.10\cdot10^9$	$5.6\cdot10^8$
	0.8	0.058	$3.24\cdot10^8$	$8.8\cdot10^7$
		0.063	$7.73\cdot10^8$	$1.1\cdot10^8$
		0.068	$1.42\cdot10^9$	$1.5\cdot10^8$
0.05 M $Bi(ClO_4)_3$ + 1 M $HClO_4$	0.3	0.044	$1.79\cdot10^5$	$3.8\cdot10^6$
		0.049	$4.25\cdot10^7$	$5.8\cdot10^7$
		0.054	$5.78\cdot10^9$	$6.8\cdot10^8$

siderations in [1, 35], one would expect the increase in N_{crit} to be formally possible when the bulk c of Bi^{3+} is lowered. Clearly, this suggestion remains to be studied additionally in a further investigation.

The other parameters of Bi nuclei formation onto the pc Pt electrode in Bi^{3+} perchlorate solution are given in Table.

CONCLUDING REMARKS

The potentiostatic current–time transients showed that the early stages of bismuth electrodeposition onto the smooth polycrystalline platinum electrode from acidic Bi^{3+} perchlorate solution rather well fit the 3D progressive nucleation and growth under diffusion control model.

Three additional points are worth noting. Firstly, under certain conditions of electrolysis, two waves in the current–time transient can be observed. Secondly, the evaluation of the diffusion coefficient for a Bi^{3+} ion leads to significantly diminished values of this parameter. This finding remains to be explained. Finally, some parameters of Bi nuclei formation depend on the value of the starting potential E_{start} in the underpotential range, as might be hoped for. Moreover, they also depend, even to the governing extent, on the range of the Pt potentials within which processes of different nature can be dominant (*viz*. the Bi UPD, reduction of surface platinum oxide occurring simultaneously with the reduction of irreversibly adsorbed Bi(III) species or irreversible adsorption of the latter). To such parameters belong the nucleation rate aN_0 and the critical number of atoms in the stable Bi nucleous N_{crit}.

Received
24 January 2000

References

1. E. Budevski, G. Staikov and W. J. Lorenz, *Electrochemical Phase Formation and Growth,* VCH, Weinheim-New York–Basel–Cambridge–Tokyo (1996).
2. D. M. Kolb, in *Advances in Electrochemistry and Electrochemical Engineering,* Vol. 11 (Eds. H. Gerischer and Ch. W. Tobias), p. 125, John Wiley & Sons, New York–Chichester–Brisbane–Toronto (1978).
3. R. R. Adžić, in *Advances in Electrochemistry and Electrochemical Engineering,* Vol. 13 (Ed. H. Gerischer), p. 159, John Wiley & Sons, New York–Chichester–Brisbane–Toronto–Singapore (1984).
4. G. Kokkinidis, *J. Electroanal. Chem.,* **201**, 217 (1986).
5. K. Jüttner, *Electrochim. Acta*, **31**, 917 (1986).
6. O. A. Petrii and A. S. Lapa, in *Itogi nauki i tekhniki. Ser. – Elektrokhimiya*, Vol. 24 (Ed. Y. M. Polukarov), p. 94, VINITI, Mocow (1987) (in Russian).
7. B. J. Bowles, *Electrochim. Acta*, **15**, 737 (1970).
8. F. Mikuni and T. Takamura, *Denki Kagaku*, **39**, 579 (1971).
9. S. H. Cadle and St. Bruckenstein, *Anal. Chem.,* **44**, 1993 (1972).
10. R. R. Adžić, D. N. Simić, A. R. Despić and D. M. Dražić, *J. Electroanal. Chem.,* **65**, 587 (1975).
11. S. Szabo and F. Nagy, *J. Electroanal. Chem.,* **70**, 357 (1976).
12. N. Furuya and S. Motoo, *J. Electroanal. Chem.,* **98**, 189 (1979).
13. I. Fonseca, J. Lin-Cai and D. Pletcher, *J. Electroanal. Chem.,* **130**, 2187 (1983).
14. R. R. Adžić and N. N. Marković, *Electrochim. Acta*, **30**, 1473 (1985).
15. J. Clavilier, J. M. Feliu and A. Aldaz, *J. Electroanal. Chem.,* **243**, 419 (1988).
16. J. Clavilier, J. M. Feliu, A. Fernandez-Vega and A. Aldaz, *J. Electroanal. Chem.,* **269**, 175 (1989).
17. R. Gómez, A. Fernandez-Vega, J. M. Feliu and A. Aldaz, *J. Phys. Chem.,* **97**, 4769 (1993).
18. M. R. Evans and G. A. Attard, *J. Electroanal. Chem.,* **345**, 337 (1993).
19. C. P. Wilde and M. Zhang, *Langmuir,* **10**, 1600 (1994).
20. R. Gómez, J. M. Feliu and A. Aldaz, *Electrochim. Acta*, **42**, 1675 (1997).
21. U. W. Hamm, D. Kramer, R. S. Zhai and D. M. Kolb, *Electrochim. Acta*, **43**, 2969 (1998).
22. A. Steponavičius and L. Gudavičiūtė, *Chemija (Vilnius)* **12** (1), 31 (2001).
23. Ch. F. Baes and R. E. Mesmer, *The Hydrolysis of Cations,* p. 375, John Wiley & Sons, New York–London–Sydney–Toronto (1976).
24. T. Biegler, D. A. J. Rand and R. Woods, *J. Electroanal. Chem.,* **29**, 269 (1971).
25. H. Angerstein-Kozlowska, in *Comprehensive Treatise of Electrochemistry,* Vol. 9 (Eds. E. Yeager, J. O' M. Bockris, B. E. Conway and S. Sarangapani), Chapt. 2, Plenum Press, New York–London (1984).
26. D. I. Leikis, K. V. Rybalka and E. S. Sevastyanov, in *Adsorption and Electrical Double Layer*, p. 5, Nauka, Mocow (1972) (in Russian).
27. R. S. Nicholson and I. Shain, *Analyt. Chem.,* **36**, 706 (1964).
28. B. Scharifker and G. Hills, *Electrochim. Acta*, **28**, 879 (1983).
29. G. Gunawardena, G. Hills, I. Montenegro, and B. Scharifker, *J. Electroanal. Chem.,* **138**, 225 (1982).
30. H. Bort, K. Jüttner, W.J. Lorenz, G. Staikov and E. Budevski, *Electrochim. Acta*, **28**, 985 (1983).
31. W. Kautek and S. Birkle, *Electrochim. Acta*, **34**, 1213 (1989).
32. L. Simanavičius, A. Stakėnas and A. Šarkis, *Electrochim. Acta*, **42**, 1581 (1997).
33. M. E. Martins, R. C. Salvarezza and A. J. Arvia, *Electrochim. Acta*, **41**, 2441 (1996).
34. A. Milchev, S. Stoyanov and R. Kaischev, *Thin Solid Films,* **22**, 267 (1974).
35. E. B. Budevski, in *Comprehensive Treatise of Electrochemistry,* Vol. 7 (Eds. B. E. Conway, J. O' M. Bockris, E. Yeager, S. U. M. Khan and R. E. White), Chapt. 7, Plenum Press, New York–London (1983).

A. Steponavičius, L. Gudavičiūtė, V. Karpavičienė, V. Kapočius

BISMUTO NUSODINIMAS PRIEŠVOLTAŠIO IR VIRŠVOLTAŠIO ZONOJE ANT GLOTNAUS POLIKRISTALINĖS PLATINOS ELEKTRODO

S a n t r a u k a

Linijinio potencialo skleidimo, ciklinės voltamperometrijos ir potenciostatinio įjungimo metodais tirtas bismuto nusodinimas plačiame potencialų intervale, apimančiame priešvoltažio ir viršvoltažio zonas, ant glotnaus polikristalinės Pt elektrodo rūgščiuose perchloratiniuose tirpaluose. Nustatyta bismuto adsorbcijos izoterma ant Pt. Remiantis potenciostatinio įjungimo metodu gautais duomenimis, parodyta, kad Bi elektrolitinio nusodinimo ant Pt ankstyvosios stadijos gana gerai aprašomos 3D branduolių susidarymo ir difuzijos kontroliuojamo augimo progresyviuoju mechanizmu. Nustatyti kai kurie branduolių susidarymo proceso parametrai.

А. Степонавичюс, Л. Гудавичюте, В. Карпавичене, В. Капочюс

ОСАЖДЕНИЕ ВИСМУТА В ЗОНАХ НЕДОНАПРЯЖЕНИЯ И ПЕРЕНАПРЯЖЕНИЯ НА ГЛАДКОМ ЭЛЕКТРОДЕ ПОЛИКРИСТАЛЛИЧЕСКОЙ ПЛАТИНЫ

Р е з ю м е

Методами линейной развертки потенциала циклической вольтамперометрии и потенциостатического включения исследовано осаждение висмута в широком интервале потенциалов, включая зоны недонапряжения и перенапряжения, на гладком электроде поликристаллической Pt в кислых перхлоратных электролитах. Установлена изотерма адсорбции висмута на Pt. На основе данных, полученных методом потенциостатического включения, показано, что ранние стадии электролитического осаждения Bi на Pt достаточно хорошо описываются прогрессивным механизмом 3Д зародышеобразования с последующим их ростом в условиях диффузионных ограничений. Рассчитаны некоторые параметры зародышеобразования.